Geosci. Model Dev. Discuss., 8, 2053–2100, 2015
www.geosci-model-dev-discuss.net/8/2053/2015/
doi:10.5194/gmdd-8-2053-2015

Geoscientific Model Development Discussions
Open Access

This discussion paper is/has been under review for the journal Geoscientific Model Development (GMD). Please refer to the corresponding final paper in GMD if available.

Impact of climate, vegetation, soil and crop management variables on multi-year ISBA-A-gs simulations of evapotranspiration over a Mediterranean crop site

S. Garrigues[1,2], A. Olioso[1,2], D. Carrer[3], B. Decharme[3], E. Martin[3], J.-C. Calvet[3], S. Moulin[1,2], and O. Marloie[4]

[1]INRA, UMR1114 EMMAH, 84914 Avignon CEDEX 9, France
[2]Université d'Avignon et des Pays de Vaucluse, UMR1114 EMMAH, 84000 Avignon, France
[3]CNRM-GAME, UMR3589, Météo-France, CNRS, Toulouse, France
[4]URFM, INRA, Avignon, France

Received: 19 December 2014 – Accepted: 26 January 2015 – Published: 26 February 2015

Correspondence to: S. Garrigues (sebastien.garrigues@paca.inra.fr)

Published by Copernicus Publications on behalf of the European Geosciences Union.

Abstract

Generic land surface models are generally driven by large-scale forcing datasets to describe the climate, the surface characteristics (soil texture, vegetation dynamic) and the cropland management (irrigation). This paper investigates the errors in these forcing variables and their impacts on the evapotranspiration (ET) simulated from the Interactions between Soil, Biosphere, and Atmosphere (ISBA-A-gs) land surface model over a 12 year Mediterranean crop succession. We evaluate the forcing datasets used in the standard implementation of ISBA over France where the model is driven by the SAFRAN high spatial resolution atmospheric reanalysis, the Leaf Area Index (LAI) cycles derived from the Ecoclimap-II land surface parameter database and the soil texture derived from the French soil database. For climate, we focus on the radiations and rainfall variables and we test additional datasets which includes the ERA-Interim low spatial resolution reanalysis, the Global Precipitation Climatology Centre dataset (GPCC) and the MeteoSat Second Generation (MSG) satellite estimate of downwelling shortwave radiations. The methodology consists in comparing the simulation achieved using large-scale forcing datasets with the simulation achieved using local observations for each forcing variable. The relative impacts of the forcing variables on simulated ET are compared with each other and with the model uncertainties triggered by errors in soil parameters.

LAI and the lack of irrigation in the simulation generate the largest mean deviations in ET between the large-scale and the local-scale simulations (equivalent to 24 and 19 months of ET over 12 yr). The climate induces smaller mean deviations equivalent to 7–8 months of ET over 12 yr. The soil texture has the lowest impact (equivalent to 3 months of ET). However, the impact of errors in the forcing variables is smaller than the impact triggered by errors in the soil parameters (equivalent to 27 months of ET). The absence of irrigation which represents 18 % of cumulative rainfall over 12 years induces a deficit in ET of 14 %. It generates much larger variations in incoming water for the model than the differences in rainfall between the reanalysis datasets. ET simulated

with the Ecoclimap-II LAI climatology is overestimated by 18 % over 12 years. This is related to the overestimation of the mean LAI over the crop cycle which reveals inaccurate representation of Mediterranean crop cycles. Compared to SAFRAN, the use of the ERA-I reanalysis, the GPCC rainfall and the downwelling shortwave radiation derived from the MSG satellite have little influence on the ET simulation performances. The error in yearly ET is mainly driven by the error in yearly rainfall and to a less extent by radiations. The SAFRAN and MSG satellite shortwave radiation estimates show similar negative biases (−9 and −11 $W m^{-2}$). The ERA-I bias in shortwave radiations is 4 times smaller at daily time scale. Both SAFRAN and ERA-I underestimate longwave downwelling radiations by −12 and −16 $W m^{-2}$, respectively. The biases in shortwave and longwave radiations show larger inter-annual variation for SAFRAN than for ERA-I. Regarding rainfall, SAFRAN and ERA-I/GPCC are slightly biased at daily and longer time scales (1 and 0.5 % of the mean rainfall measurement). The SAFRAN rainfall estimates are more precise due to the use of the in situ daily rainfall measurements of the Avignon site in the reanalysis.

1 Introduction

Evapotranspiration (ET) is a key component of the water balance and the energy budget of land surfaces. It is an essential information to estimate air temperature and air humidity of surface boundary layer (Noilhan et al., 2011) in atmospheric models and to monitor river discharge in hydrology models (Habels et al., 2008). ET can be estimated from Land surface model (LSM) which describes the vertical exchange of energy and mass between the soil, the vegetation and the atmosphere at hourly time scale. LSMs have been designed to be coupled to atmospheric or hydrology models for large-scale studies. Uncertainties in LSM simulation of ET can be attributed to (i) model structure and parameters (referred hereafter as model uncertainties) and (ii) errors in the forcing variables used to drive the model and to integrate it spatially. The forcing variables concern the climate and the land surface characteristics. They are generally provided by large-scale datasets characterized by coarse spatial resolution (10–50 km) which may be not accurate enough to resolve the spatial and temporal variability of ET at regional scale. Long-term prediction of surface fluxes and water balance requires to characterize the impact of forcing variables on LSM simulations at seasonal and multi-annual scales.

Atmospheric reanalysis results from the combination of atmospheric models and meteorological observations. One challenge concerns the evaluation of their representativeness of regional climates (Bosilovich, 2013). Large differences among reanalysis datasets and between these datasets and in situ observations are reported in Zhao et al. (2011). The errors are the greatest at hourly and daily time steps and generally decrease at longer time scales (Zhao et al., 2011). They can be large in mountainous regions due to unresolved topography variability and lack of dense network measurements (Zhao et al., 2008; Wang et al., 2012). Air temperature is generally a robust estimate (Quintana-Seguí et al., 2008; Decker et al., 2012). Zhao et al. (2011) found median Mean Absolute Error (MAE) values ranging from 0.5 to 2 °C for 4 reanalysis datasets evaluated over 6 French sites. Rainfall and radiation are frequently reported as the most uncertain variables (Szczypta et al., 2011; Bosilovich et al., 2013). Besides, they are two main external drivers of ET (Teulling et al., 2009; Miralles et al., 2011). For rainfalls, Zhao et al. (2011) found MAE ranging from 1.8 to 4 mm day^{-1}. Reanalysis generally fails to describe the spatiotemporal heterogeneity of precipitation of Mediterranean regions where rainfalls are frequently controlled by local convective elements (Anquetin et al., 2010; Szczypta et al., 2011; Bosilovich et al., 2013). The errors in precipitation particularly affect the simulation of surface flux, soil moisture and vegetation growth which can have large impact on the simulation of hydrological variables (Decharme and Douville, 2006a; Maggioni et al., 2012; Anquetin et al., 2010). Regarding radiations, their estimates are frequently inaccurate due to the few number of in situ observations used to constraint the radiative transfer model used in the reanalysis (Carrer et al., 2012). Zhao et al. (2011) report daily MAE ranging from 20 to 60 W m^{-2} for downwelling shortwave radiations (referred as shortwave radiation or SWdown hereafter) and from 10 to 20 W m^{-2} for downwelling longwave radiations (referred as longwave radiation or LWdown). Underestimations in SWdown are frequently reported over Mediterranean regions (Quintana-Seguí et al., 2008; Szczypta et al., 2011). New radiation products derived from satellite observations, such as MSG/SEVIRI can advantageously be used over these areas that lack high-resolution meteorological measurements in order to simulate the energy budget (Carrer et al., 2012).

The representation of the surface characteristics concerns all the variables used to force the model in terms of land cover type and use, vegetation dynamic and soil properties. Since the model parameters are generally prescribed per land surface type, errors in land cover map can induce large errors in LSM outputs (Avissar and Pielke, 1989; Ge et al., 2009; Pijanowski et al., 2011). The soil texture is generally used to infer the soil hydrodynamic properties through pedotransfer functions (Espino et al., 1996; Baroni et al., 2010). It is a key variable for the spatial integration of the model since the soil properties explain a large part of ET uncertainties (Braud et al., 1995; Garrigues et al., 2015). The vegetation dynamic is represented by the Leaf Area Index (LAI) cycle. It is a key variable involved in the simulation of canopy conductance. It is used to infer secondary parameters such as the vegetation cover which controls evapotranspiration partitioning. LAI cycle can be described by a climatology or satellite observations. Several studies have reported great discrepancies between distinct LAI satellite observations (Garrigues et al., 2008; Lafont et al., 2011). Their spatial and temporal resolution may not be fine enough to represent the cropland dynamic. Garrigues et al. (2015) highlight the large impact of the succession of crop cycle and inter-crop periods on the temporal dynamic of ET over long period of time. Finally, agricultural land management such as irrigation can significantly influence the surface energy and water balance (de Rosnay et al., 2003; Olioso et al., 2005, 2013).

The ISBA-A-gs version (Calvet et al., 1998) of the Interactions between Soil, Biosphere, and Atmosphere (ISBA) model (Noilhan and Planton, 1989; Noilhan and Mahfouf, 1996) is considered in this work. ISBA relies on a single surface energy budget of a soil-vegetation composite and a force restore scheme for heat and water transfers.

GMDD
8, 2053–2100, 2015

Its A-gs component includes a coupled stomatal conductance-photosynthesis scheme. In its standard implementation over France, ISBA is driven by the SAFRAN high spatial resolution atmospheric reanalysis (Quintana-Seguí et al., 2008), the LAI cycles derived from the Ecoclimap-II land surface parameter database (Faroux et al., 2013) and the soil texture derived from the French soil database (King et al., 1995). These forcing datasets are operationally used in the SIM (SAFRAN-ISBA-MODCOU) system which is dedicated to hydrology monitoring (Habets et al., 2008; Vidal et al., 2010a) and the LDAS (Land Data Assimilation System) which combines the model and satellite observations to monitor vegetation and soil moisture (Barbu et al., 2013).

This work aims at evaluating the errors in various forcing variables and comparing their relative impacts on the ISBA-A-gs simulation of ET over a long period of time. We focus on the rainfall and the radiation climate variables, the irrigation and two key surface characteristics: the LAI cycle and the soil texture. We evaluate the forcing datasets used in the standard implementation of ISBA over France. For climate, additional datasets are tested which includes the ERA-Interim low spatial resolution reanalysis (Simmons et al., 2007), the Global Precipitation Climatology Centre dataset (GPCC, Schneider et al., 2011) and the MeteoSat Second Generation (MSG) satellite estimate of downwelling shortwave radiations (Carrer et al., 2012). These datasets are frequently used for the implementation of ISBA at the continental scale and we compared their performances with the SAFRAN reanalysis. We chose to evaluate the forcing variables over a crop site, for which the irrigation and the succession of crop and inter-crop periods are critical drivers of ET dynamics. We explicitly represent crop rotation in the simulation and we assess the impact of the forcing variables over a 12 yr crop succession which has not yet been addressed. The evaluation is done for Mediterranean climate for which the errors in the reanalysis estimates of radiation and rainfall were reported to be large (Szczypta et al., 2011). The evaluation is carried out at the Avignon site which is representative of typical Mediterranean cropland and provides 12 years of continuous measurements of micrometeorological variables and surface fluxes. The forcing variables are tested for a large range of surface and atmospheric states and are evaluated at hourly, daily and multi-year time scales. The methodology consists in comparing the simulation achieved using large-scale forcing datasets and the simulation achieved using local observations for each forcing variable. The performances of each simulation are assessed against ET measurements. The relative impacts of the forcing variables on simulated ET are compared with each other. We also evaluate how they compare to the model uncertainties triggered by errors in the soil hydrodynamic parameters.

2 Site and in situ data

2.1 Site characteristics

The forcing datasets and ET simulations are evaluated over the "Remote sensing and flux site" of INRA Avignon[1] (France, 4.8789° E, 43.9167° N; alt = 32 m a.s.l.). This site is characterized by a Mediterranean climate with a mean annual temperature of 14 °C and a mean annual precipitation of 687 mm. It is a flat agricultural field of 1.9 ha oriented north–south in the prevailing wind direction. The crop rotation during the 12 year period (Table 2, Fig. 1) consists in a succession of winter arable crops (wheat, peas) and spring/summer arable crops (Sorghum, maize, sunflower). During the inter-crop periods, the soil is mostly bare. The soil texture comprises 33 % of clay and 14 % of sand. The in situ values of the soil water content at saturation, field capacity and wilting point are 0.39, 0.31 and 0.18. More information on this site can be found in Garrigues et al. (2015).

2.2 Field measurements

Half-hourly observations of the main climatic variables, the shortwave and longwave radiation fluxes, the turbulent heat fluxes, the ground heat flux, and the soil moisture

[1] https://www4.paca.inra.fr/emmah_eng/Facilities/In-situ-facilities/Remote-Sensing-Fluxes.

Discussion Paper | Discussion Paper | Discussion Paper | Discussion Paper |

GMDD
8, 2053–2100, 2015

Impact of forcing variables on ISBA-A-gs simulation of ET
S. Garrigues et al.
Title Page
Abstract | Introduction
Conclusions | References
Tables | Figures
◀◀ | ▶▶
◀ | ▶
Back | Close
Full Screen / Esc
Printer-friendly Version
Interactive Discussion

have been continuously monitored since 2001. The latent heat flux (LE) was measured with an eddy-covariance system. The latter was composed of a 3-D sonic anemometer set up in 2001 and of an open-path gas (H_2O, CO_2) analyzer set up in November 2003. The system was monitored following the state of the art guidelines for cropland sites (Rebmann et al., 2012; Moureaux et al., 2012). Fluxes were computed on 30 min intervals using the EDIRE software[2]. The flux data processing included spike detection on raw data and standard eddy-covariance corrections. The ECPP (Eddy Covariance Post Processing) software (Beziat et al., 2009) was used to discard spurious flux and to apply the Foken et al. (2004) quality control. In this work, only the best quality class of data (Mauder et al., 2013) was used. An additional threshold of 100 $W\,m^{-2}$ on the energy balance non-closure was applied to eradicate very inconsistent fluxes. The mean and the SD of the absolute value of the energy balance non-closure are 28 and 22 $W\,m^{-2}$, respectively, which is comparable to the non-closure reported for cropland in Wilson et al. (2002), Hendricks Franssen et al. (2010) and Ingwersen et al. (2010). Direct measurements of LE were used over the 20 November 2003–26 June 2012 period. The percentage of valid measurement was 47 % (55 % for daytime). For the 2001–2003 period, LE estimates were derived as the residual of the energy balance.

The crop characteristics (LAI, height, biomass) were regularly measured at selected phenological stages. The vegetation height was linearly interpolated on a daily basis. Daily interpolation of LAI was achieved using a functional relationship between LAI and the sum of degree days (Duveiller et al., 2011).

3 The ISBA-A-gs model

The ISBA model (Noilhan and Planton, 1989; Noilhan and Mahfouf, 1996) is developed at the CNRM/Météo-France within the SURFEX surface modeling platform (Masson

[2]Robert Clement, ©1999; University of Edinburgh, UK, http://www.geos.ed.ac.uk/abs/research/micromet/EdiRe.

GMDD
8, 2053–2100, 2015
Impact of forcing variables on ISBA-A-gs simulation of ET
S. Garrigues et al.

et al., 2013). In this study, we used the version 6.1 of SURFEX. ISBA relies on a single surface energy budget of a soil-vegetation composite. Separate soil evaporation and transpiration fluxes are simulated. In this work, the soil water transfers are simulated using a force-restore scheme. They are represented by the time course of the volumetric soil moisture of three reservoirs: the superficial reservoir of thickness $d_1 = 0.01$ m to regulate the soil evaporation, the root-zone (from the surface to a depth d_2) and the deep reservoir which extends from the base of the root-zone to the total soil column depth (d_3). Regarding the vegetation processes, we used the A-gs version of ISBA (Calvet et al., 1998, 2008). It simulates the photosynthesis and computes the stomatal conductance as a function of the net assimilation of CO_2. The simulation of the plant response to drought relies on distinct evolutions of the water use efficiency and is parameterized as a function of the maximum root-zone water stock available for the plant (Calvet et al., 2012). The model is parametrized and run for 12 generic land surface homogeneous patches which includes 9 types of vegetation.

In this work, ISBA-A-gs does not simulate the vegetation dynamic and the LAI cycle is provided as a forcing variable. The irrigation was not simulated by the model and is also considered as a forcing variable. In Sect. 7, the irrigation module of the model is tested and discussed. The soil depths and the vegetation parameters are given by the Ecoclimap-II land surface parameter database described below. The soil parameters are derived from soil texture using the pedotransfer functions embedded in the model which rely on the Clapp and Hornberger (1978) soil texture classification (Noilhan and Lacarrère, 1995).

GMDD
8, 2053–2100, 2015

4 Forcing datasets

4.1 Climate datasets

4.1.1 SAFRAN reanalysis

The SAFRAN dataset is produced by the French Meteorological Service (Météo-France). It provides a reanalysis of the climate variables at 8 km horizontal spatial resolution and hourly time scale over France back to 1958 (Quintana-Seguí et al., 2008; Vidal et al., 2010b). The reanalysis is performed over climatically homogeneous zones covering the French territory. Vertical profiles (vertical resolution of 300 m) of temperature, humidity and wind speed are computed every 6 h from optimal interpolation between the simulations from an atmospheric model (ARPEGE model with a spatial resolution of ~ 20–30 km; Déqué et al., 1994) and the available in situ observations (acquired by ~ 600 stations over France). The downwelling shortwave and longwave radiations are derived from a radiative transfer scheme which is not constrained by observations (Ritter and Geleyn, 1992). The precipitation is computed on a daily basis from optimal interpolation between a climatology and the rain gauge observations within the climatic zone. All analyzed variables are temporally interpolated to hourly values using physical constraints. They are projected over an 8 km Lambert grid. For temperature, humidity, wind speed and radiation variables, it consists in affecting to each grid cell the value of the vertical profile of the variable at the elevation of the grid cell.

4.1.2 ERA-Interim reanalysis

The ERA-Interim (ERA-I) reanalysis is produced by ECMWF (European Center for Medium-Range Weather Forecasts) at a spatial resolution of 0.5° and a 3 h time step. The reanalysis is based on a 4-D-VAR data assimilation scheme using the meteorological observations within a 03:00–15:00 UTC window (Simmons et al., 2007). Poor

GMDD
8, 2053–2100, 2015

Impact of forcing variables on ISBA-A-gs simulation of ET

S. Garrigues et al.

performances have been reported for ERA-I rainfall (Szczypta et al., 2011). For the ISBA implementation at continental scale, the ERA-I rainfall is corrected using the Global Precipitation Climatology Centre dataset (GPCC v6, Schneider et al., 2011). The latter provides monthly quality-controlled precipitation totals from 1901 to present which were derived from data from 67 200 rain gauge stations world-wide. The GPCC-corrected ERA-I rainfall will be denoted ERA-I/GPCC hereafter.

4.1.3 MSG satellite downwelling shortwave radiation

In the framework of the Land Surface Analysis Satellite Application Facility (LSA SAF), downwelling shortwave radiation is derived from the Spinning Enhanced Visible and Infrared Imager (SEVIRI) instrument on board the MeteoSat Second Generation (MSG) satellite at a temporal frequency of 30 min and a spatial resolution of 3 km. This dataset is available at http://landsaf.meteo.pt. The product characteristics and the estimation method are given in Geiger et al., 2008 and Carrer et al., 2012. Under cloudy-sky conditions, shortwave radiation is estimated using the strong anti-correlation between the reflectance measured by the satellite and the solar radiation reaching the ground. Under clear-sky conditions, shortwave radiation is estimated using an atmospheric transmittance model (Geiger et al., 2008). The MSG satellite dataset is available from 12 October 2004. Before this date, the SAFRAN shortwave radiation is used. Missing MSG data represents 7 % of the 12 October 2004–26 June 2012 period. They were replaced by the SAFRAN estimates. The MSG estimate of downwelling longwave radiation was not available for this work. Carrer et al., 2012 showed that this product has no significant impact on the scores of the ISBA simultations and that the MSG shortwave radiation has the largest added-value.

4.2 Surface characteristic datasets

The surface parameters of ISBA-A-gs are given by the Ecoclimap II database (Gibelin et al., 2006; Faroux et al., 2013). The latter provides land surface parameters for ∼ 273 distinct land covers over Europe at 1 km resolution. Ecoclimap-II provides a monthly LAI climatology obtained from the analysis of the MODIS satellite observations over each land cover and land surface patch of the model (Faroux et al., 2013). For crops, the fraction of vegetation cover and the vegetation height are derived using empirical functions of LAI (Masson et al., 2004). The surface parameters and the LAI cycles are derived for each land surface patch of the model. The model provides outputs at the surface patch scale which are aggregated at 1 km resolution using the proportion of each land surface patch within the 1 km grid cell.

In the standard implementation of the model over France, the soil texture is provided by the French soil database on a 1 : 1 000 000 scale map (King et al., 1995) which has been resampled over the SAFRAN grid at a 8 km resolution (Habets et al., 2008).

5 Methodology

5.1 Model implementation at the Avignon site

ISBA-A-gs was run at a 5 min time step. 30 min outputs of the state variables were analyzed. Continuous simulations were performed from 25 April 2001 up to 26 June 2012. The simulation was initialized once on 25 April 2001 using in situ soil temperature and soil moisture measurements. The succession of crop and inter-crop periods is explicitly represented in the simulations which is illustrated in Fig. 1. In this work, we analyze the model's outputs at the land surface patch scale of the model. We do not consider the outputs aggregated at 1 km resolution which does not match the field scale. The C3 crop patch was used to represent wheat, pea, and sunflower. The C4 crop patch was used for maize and Sorghum. Inter-crop periods are represented by the bare soil patch.

GMDD
8, 2053–2100, 2015
Impact of forcing variables on ISBA-A-gs simulation of ET
S. Garrigues et al.

Title Page
Abstract Introduction
Conclusions References
Tables Figures
◀ ▶
◀ ▶
Back Close
Full Screen / Esc
Printer-friendly Version
Interactive Discussion

5.2 Experimental design

This work aims at evaluating the impact of errors in large-scale forcing variables on simulated ET. We chose to test the climate with a focus on the rainfall and the radiation drivers, the irrigation and two key surface characteristics: the soil texture and the LAI cycle. For each forcing variable, the simulations achieved with the large-scale datasets are compared to the simulations achieved with the local observations taken at the Avignon site. Distinct simulations were designed (Table 3).

4 simulations were achieved using large-scale datasets for all the tested forcing variables. Soil texture was derived from the French soil database. LAI and vegetation height were derived from Ecoclimap-II. No irrigation was accounted for. These simulations differ only by the climate dataset:

- S_{SAF} was conducted with the SAFRAN climate.
- S_{ERA} was conducted with the ERA-I climate.
- S_{GPCC} was conducted with the SAFRAN climate where rainfall were replaced by the ERA-I/GPCC rainfall.
- S_{MSG} was conducted with the SAFRAN climate where downwelling shortwave radiations were replaced by the MSG satellite shortwave radiations.

The other simulations were achieved by replacing the large-scale dataset used for each forcing variable by the corresponding local observations taken at the Avignon site. This was done consecutively for climate, irrigation, soil texture and vegetation dynamic as indicated in Table 3. We obtained the 4 following simulations:

- S_{clim} was conducted with the in situ climate (denoted "clim"). Irrigation was not accounted for and large-scale datasets were used for soil texture and vegetation.
- $S_{\text{clim, irri}}$ was conducted with the in situ climate and the in situ irrigation (denoted "irri"). Large-scale datasets were used for soil texture and vegetation dynamic.

GMDD
8, 2053–2100, 2015

- $S_{\text{clim, irri, text}}$ was conducted with the in situ climate, the in situ irrigation and the in situ soil texture (denoted "text"). Large-scale dataset was used for the vegetation dynamic.
- $S_{\text{clim, irri, text, veg}}$ was conducted with the in situ climate, the in situ irrigation, the in situ soil texture, and the in situ vegetation dynamic ("veg").

We investigate the impact of:

- *the climate*: we compare the simulations forced by the distinct large-scale climate datasets (S_{SAF}, S_{ERA}, S_{GPCC}, S_{MSG}) with the simulation achieved with the in situ meteorological observations (S_{clim}). We test:
    - the *reanalysis dataset* comparing S_{SAF} with S_{ERA}.
    - the *rainfall dataset* comparing S_{SAF} with S_{GPCC}.
    - the satellite *estimate of shortwave radiation* comparing S_{SAF} with S_{MSG}.
- *the absence of irrigation*: we compare S_{clim} achieved without irrigation with $S_{\text{clim, irri}}$ where the local irrigation amount was added to rainfall.
    - *the soil texture*: we compare $S_{\text{clim, irri}}$ achieved with the texture from the French soil database and $S_{\text{clim, irri, text}}$ achieved using the local soil texture,
    - *the vegetation dynamic*: we compare $S_{\text{clim, irri, text}}$ forced with the Ecoclimap-II monthly LAI and vegetation height with $S_{\text{clim, irri, text, veg}}$ forced with the in situ LAI and vegetation height averaged over 10-days.

To compare the uncertainties triggered by the forcing variables with those generated by errors in the soil hydrodynamic parameters, the control simulation S_{CTL} was achieved using local forcing and in situ values for the soil moisture at saturation, the soil moisture at field capacity and the soil moisture at wilting point. Garrigues et al. (2015) showed that these parameters drive a large part of the uncertainties in simulated ET. S_{CTL} is compared with $S_{\text{clim, irri, text, veg}}$ which was achieved using the ISBA pedotransfer estimates of these parameters.

GMDD
8, 2053–2100, 2015

5.3 Simulation evaluation metrics

ET simulations are evaluated using LE (in $W\,m^{-2}$) computed at half-hourly time scale and cumulative ET (in mm) computed at daily and 12 yr time scales. The impact of using large-scale forcing variables on ET simulation is quantified through two distinct evaluation efforts.

The first one concerns the comparison of the simulation achieved with large-scale forcing variable and the simulation based on local observations. We used the correlation coefficient (r), the Root Mean Square of the Difference (RMSD), the Mean Difference (MD) and the SD of differences (SDD) between the simulations. The RMSD quantifies the total discrepancies. MD quantifies systematic differences while SDD represents random scattering between the simulations.

The second effort consists in evaluating the performance scores of each simulation against eddy covariance measurements. We used the Root Mean Square Error (RMSE), the bias between the simulation and the measurement (BIAS), the SD of the differences between the simulation and the measurement (SDD) and the Nash index (NI, Nash and Sutcliffe, 1970). The bias quantifies the accuracy of the simulation while SDD is an indication of the precision of the simulation. The performance scores were computed over the 20 November 2003–26 June 2012 period for which direct LE measurements were available. For comparison with measurements, daily ET was computed over daytime when a minimum of 90 % of daytime time steps were valid. Uncertainties in the eddy-covariance measurements are not explicitly considered in this analysis. As discussed in Garrigues et al. (2015), they mainly explain the random differences between the simulation and the measurement.

We also evaluate the performance scores (r, BIAS, SDD) of the climate variables (rainfall and radiations) against meterorological observations taken at the Avignon site.

6 Results:

Figure 2 shows the differences in cumulative ET between the simulation achieved with large-scale forcing datasets and the simulation performed with local observations for the climate, the irrigation, the soil texture and the vegetation dynamic, over the 2001–2012 period. The differences between the simulation achieved with the pedotransfer estimates of the soil parameters and the simulation based on the in situ values is presented and represents the impact of errors in model parameters. Table 4 reports the metrics which quantifies the scattering in ET simulated with large-scale vs. local forcing. Table 5 gives the performance scores of each simulation. Tables 4 and 5 show similar responses to the tested forcing variables for LE at half-hourly time scale, daily ET and 12 yr ET. The following analysis is based on daily ET and 12 yr ET and is transferable to LE. The following sub-sections describe the results for each forcing variable and the comparison of their relative impact on ET is discussed in Sect. 7.

6.1 Impact of climate variables

The use of the SAFRAN climate in S_{SAF} decreases the cumulative ET over 12 years by 343 mm (6 %) compared to the local climate simulation (S_{clim}). This represents 8 months of ET. The use of the ERA-I/GPCC climate in S_{ERA} generates larger random scattering with S_{clim} for daily ET but leads to slightly reduced MD (−286 mm equivalent to 7 months of ET). Regarding the simulation performances, the use of ERA-I/GPCC decreases NI and increases RMSE (Table 5).

The use of the ERA-I/GPCC rainfall in S_{GPCC} instead of the SAFRAN rainfall slightly increases ET random scattering with S_{clim} and does not affect MD (Table 4). It slightly reduces the simulation performance scores (Table 5). Table 6 indicates that the ERA-I/GPCC and the SAFRAN rainfall have very low biases at daily and longer time steps (0.5 and 1 % of the mean measurement). Poor correlation and large SDD are found at 3 h time scale. Correlation increases and relative SDD decreases at daily time scale. This effect is more pronounced for the SAFRAN rainfall (relative SDD is divided by

GMDD
8, 2053–2100, 2015

7.5 between 3 h and daily time step) than for the ERA-I/GPCC rainfall (relative SDD is divided by 2.5 between 3 h and daily time step). At longer time steps, relative SDD of both datasets decays at a rate which is consistent with the change of time support. At daily and longer time scales, SDD of the ERA-I/GPCC rainfall are 3 times larger than the SAFRAN ones and the biases are about half of the SAFRAN ones. Figure 3 shows that the ERA-I/GPCC rainfall is overestimated in winter and underestimated in spring and summer.

The use of the shortwave radiation derived from the MSG satellite in S_{MSG} instead of the SAFRAN estimate does not significantly impact ET (Tables 4 and 5). We verified that the metrics computed over the complete 2001–2012 period in Table 4 and 5 provide similar results than the metrics computed over the 12 October 2004–26 June 2012 period over which the satellite shortwave radiation is used instead of the SAFRAN estimate. The comparison with measured shortwave radiation shows similar negative biases ($\sim -10\,\mathrm{W\,m^{-2}}$) and SDD for SAFRAN and MSG at both half-hourly and daily time scales (Table 7). The SAFRAN shortwave radiation is underestimated at midday in summer while the satellite estimate is underestimated in the afternoon. The ERA-I shortwave radiation has an absolute bias 4 times smaller than SAFRAN. It is underestimated in the morning and overestimated in the afternoon (Fig. 4). SAFRAN and ERA-I underestimate longwave radiation by -12 and $-16\,\mathrm{W\,m^{-2}}$ (Table 7). Figure 5 shows that SAFRAN describes an inverse diurnal cycle of longwave radiation and underestimates the maximum value in the afternoon. ERA-I shows consistent diurnal variations but it is marked by a large negative bias through the diurnal and the seasonal cycles. The biases in shortwave and longwave radiations translate in biases in simulated net radiation which is overestimated using the ERA-I climate and underestimated with the SAFRAN climate (Table 7).

Figure 6 displays the errors in yearly rainfall and radiation for the SAFRAN and ERA-I/GPCC reanalyses along with their impact on yearly ET. SAFRAN and ERA-I/GPCC have contrasted inter-annual evolutions of yearly budgets. For SAFRAN, the yearly rainfall error shows low inter-annual variation and ranges from -42 to 32 mm. The er-

GMDD
8, 2053–2100, 2015

rors in yearly shortwave and longwave radiations show greater inter-annual variations and range from −661 to −21 MJ and from −548 to −107 MJ, respectively. For ERA-I/GPCC, the yearly rainfall error is frequently larger than SAFRAN and shows larger inter-annual variability (−81 to 98 $mm\,yr^{-1}$). The ERA-I errors in yearly shortwave and longwave radiations are steadier than SAFRAN and vary from −52 to 179 MJ and from −625 to −385 MJ, respectively. This is related to the smaller SDD reported for ERA-I radiations at daily time scale (Table 7). The differences in yearly ET between the reanalyses and the local climate simulations fall within similar range of values (from −82 to 3 $mm\,yr^{-1}$ for SAFRAN and from −93 to 12 $mm\,yr^{-1}$ for ERA-I/GPCC). Figure 6 shows that the evolution of the error in yearly ET is mainly related to the errors in rainfall. This particularly holds true for GPCC. The impacts of radiations are smaller except in 2008 and 2010 for SAFRAN.

6.2 Impact of irrigation

The lack of irrigation in S_{clim} decreases the cumulative ET by 973 mm over 12 years (14 %, equivalent to 19 months of ET) compared to $S_{\text{clim, irri}}$ for which the irrigation amount was added to the local rainfall. MD in ET between S_{clim} and $S_{\text{clim, irri}}$ is about 3 times MD between the SAFRAN and the local climate simulations. Accounting for the irrigation triggers the largest bias reduction with the measurements among the forcing variables (Table 5: reduction of 70 % for daily ET). Irrigation and rainfall amount to 1295 and 7138 mm over 12 years. Figure 3 shows a large increase in cumulative amount of water in May–July due to irrigation which is related to the decreases in ET observed for irrigated summer crops in Fig. 2 (brown curve).

6.3 Impact of soil texture

The use of the soil texture derived from the large-scale French soil database in $S_{\text{clim,irri}}$ decreases the cumulative ET over 12 years by 156 mm (2 %, equivalent to 3 months of ET) compared to $S_{\text{clim, irri, text}}$ achieved with the local soil texture.

GMDD
8, 2053–2100, 2015

6.4 Impact of vegetation dynamic

The use of the Ecoclimap-II LAI climatology in $S_{\text{clim, irri, text}}$ increases the cumulative ET over 12 years by 1063 mm (18 %, equivalent to 24 months of ET) compared to $S_{\text{clim, irri, text, veg}}$ achieved with in situ LAI and vegetation height measurements. This is related to the overestimation of the Ecoclimap-II LAI over the crop cycle (bias of $\sim 1\,\text{m}^2\,\text{m}^{-2}$). Figure 7 shows that Ecoclimap-II overestimates low LAI during the early and late stages of the crop cycle. However, it frequently underestimates the maximum LAI for wheat crops (e.g. 2002, 2004, 2006) which explains the local decrease in ET observed for these crop cycles in Fig. 2 (blue curve). Ecoclimap-II shows incorrect decrease in LAI at the early stages of wheat crops (e.g. wheat in 2002). The maximum LAI of wheat crops is late compared to measurements. The timing of maximum LAI is in better agreement with the measurements for summer crops (e.g. Sorghum in 2007 and 2009).

7 Discussion

7.1 Hierarchy of the impacts of the forcing errors

LAI and the lack of irrigation generate the largest mean deviations in ET between the large-scale and the local forcing simulations (equivalent to 24 and 19 months of ET over 12 yr). The climate induces mean deviations 3 up to 4 times smaller (equivalent to 7–8 months of ET over 12 yr). The soil texture has the lowest impact (equivalent to 3 months of ET). However, the impact of the forcing variables is smaller than the impact of the soil hydrodynamic parameters (equivalent to 27 months of ET).

Changing the climate forcing dataset has little influence on ET simulation compared to the impact of vegetation and irrigation forcing variables. The use of the ERA-I climate and the GPCC rainfall slightly decreases the precision in simulated ET compared to the SAFRAN simulation. But the accuracy is unchanged. The use of shortwave radiation derived from the MSG satellite does not improve the ET simulation performances compared to the SAFRAN simulation. When considering yearly values, the error in yearly ET is mainly driven by the errors in yearly rainfall and to a less extent by the errors in radiations.

The biases in ET generated by the large-scale forcing variables are lower than those triggered by the soil parameters. The use of the in situ soil parameters reduces the biases by 74 % for daily ET. In the standard implementation of the model, the soil parameters are derived from the ISBA pedotransfer functions. The latter were proved to be inaccurate for the site under study (Garrigues et al., 2015). The overestimation of the soil moisture at saturation triggers an underestimation of the soil evaporation during the wet bare soil periods. The overestimation of the soil moisture at wilting point leads to the underestimation of the water stock available for the crop's growth and the resulting transpiration is underestimated.

This work highlights error compensations between the biases induced by the forcing variables and the biases due to the errors in the model parameters. The overestimation of the Ecoclimap-II LAI cancels out part of the underestimation in ET triggered by the soil parameters. This leads to apparent higher performance scores for the $S_{\text{clim, irri, text}}$ simulation based on Ecoclimap-II LAI than the simulation $S_{\text{clim, irri, text, veg}}$ based on local LAI (Table 5).

7.2 Analysis of the errors in the forcing variables

7.2.1 Irrigation

Irrigation is a key component of the water balance of Mediterranean cropland. It represents 18 % of cumulative rainfall over 12 year for this site. It concerns summer crops and thus affects ET from May to July. It induces much larger variation in input water for the model than the differences in rainfall estimates between reanalysis datasets. It significantly increases evapotranspiration locally that could affect local climate (Len et al., 2013). However accurate information on irrigation amount is rarely available over large areas. A possible strategy consists in simulating the irrigation amount required to satisfy crop water needs. But one can wonder whether LSM irrigation models are representative of actual irrigation practices. An irrigation model has been implemented in ISBA-A-gs for C4 irrigated crops (Calvet et al., 2008). It consists in adding an amount of 30 mm to the precipitation each time the simulated soil water content available for the crop reaches a predefined threshold (Calvet et al., 2008). We tested this model for the irrigated crops of this experiment. The results are reported in Table 2. The simulated irrigation amounts are largely overestimated except for maize in 2001 and Sorghum in 2009 which have more realistic estimates. Bias and SDD computed over 8 crop cycles are 108 and 134 mm. Figure 8 shows accurate monthly irrigation estimates in April and May, unrealistic estimates during crop senescence in August and frequent overestimation of the inter-annual variability. The soil moisture thresholds used to trigger irrigation are probably too high for this experiment and need to be adapted for Mediterranean crops. Constraints on the irrigation period and the irrigation amount need to be incorporated to better represent the actual agricultural practices. Adding the amount of irrigation water to rainfall may not be adapted for all types of irrigations (pressurized vs. gravity distribution).

7.2.2 Vegetation dynamic

The Ecoclimap-II LAI climatology is derived from the 2002–2006 MODIS satellite observations at 1 km spatial resolution. The first explanation of the differences between the Ecoclimap-II LAI and the local LAI is the spatial and the temporal mismatch between the satellite observations and the local field. The 1 km satellite pixel is composed of bare soil and vegetation surfaces. Consequently, the maximum LAI of Ecoclimap-II is reduced compared to that of the field measurement. This can explain the ET underestimation observed at the vegetation peak for wheat crops. The satellite observations comprise a mix of crops with possibly distinct cycles. Therefore, a particular crop cycle cannot be represented, nor the local crop rotation. The monthly time step of Ecoclimap-II can be too coarse to properly resolve the changes in crop phenology which explains

GMDD
8, 2053–2100, 2015

the frequent inaccurate timing of the Ecoclimap-II maximum LAI. The second explanation of the differences between the Ecoclimap-II and the local LAI is related to the intrinsic uncertainties of the Ecoclimap-II LAI. Ecoclimap-II shows unrealistic crop cycle compared to the local LAI measurements which are representative of typical crop cycles of the studied region. As a climatology, it does not resolve the inter-annual variability. The absence of discrimination between winter and summer crop patches hampers the proper representation of crop succession. The inter-crop periods during which the surface can be bare during long period of time (up to 9 months in this experiment) are not represented. This leads to an underestimation of the bare soil surfaces and an overestimation of ET simulated over a long period of time.

7.2.3 Soil texture

While the clay and sand fractions given by the French soil database are significantly different from the local values, the impact on ET is low. Soil texture is used in the model to infer the values of the soil hydrodynamic parameters. Table 3 shows that the use of the large-scale soil texture and the local soil texture lead to similar values of the soil moisture at saturation and the maximum water stock available for the crop (MaxAWC). These parameters are key drivers of the simulation of soil evaporation and transpiration, respectively. The steady MaxAWC is a consequence of the quasi-parallel shapes of the ISBA pedotransfer functions used to estimate the soil moisture at field capacity and wilting point (Noilhan and Lacarrère, 1995). This highlights the limit of these pedotransfer functions to reproduce the spatial variability of the soil hydrodynamic properties across various soil types.

7.2.4 Climate

Regarding radiations, the underestimation of shortwave radiation by SAFRAN at midday in summer is in agreement with the Carrer et al. (2012)'s results. ERA-I shows a lower bias due to compensation effects through the diurnal cycle. This confirms the

GMDD
8, 2053–2100, 2015

better performance scores of daily shortwave radiation reported for ERA-I in Szczypta et al. (2011). Both SAFRAN and ERA-I underestimates longwave radiation. The biases in shortwave and longwave radiations show large inter-annual variability for SAFRAN, that may hamper their proper correction. The uncertainties in the reanalysis estimates of shortwave and longwave radiations are attributed to shortcomings in the radiative transfer scheme and to an insufficient number of observations to constrain the reanalysis. Conversely to Carrer et al. (2012), our work does not show higher levels of accuracy and precision for the MSG satellite estimates of shortwave radiations. The latter are underestimated in the afternoon which leads to slightly larger bias than SAFRAN. This can be related to the high occurrence of clear-sky conditions at the Avignon site for which the satellite measurements are not explicitly used. The clear-sky algorithm relies on an empirical parametrization of the atmospheric transmittance and on a climatology for the aerosol content. This may not be accurate enough to resolve the large variations in the aerosol content generated by the frequent strong wind conditions in the Avignon region. Besides, possible errors in the cloud mask used to trigger the clear-sky/cloudy-sky retrieval algorithm can have a large impact on shortwave radiation estimates (Geiger et al., 2008).

Regarding rainfall, the SAFRAN estimates are more precise than the ERA-I/GPCC estimates at daily and longer time scales. ERA-I/GPCC shows large inter-annual variability in yearly rainfall error which can reach up to 100 mm. The use of the in situ daily rainfall measurements of the Avignon site in the SAFRAN reanalysis may explain its higher precision (Quintana-Seguí et al., 2008). The rainfall estimates of both datasets are more uncertain at hourly time scale which reveals shortcomings in the rescaling of daily values to hourly values.

7.2.5 Impact of spatial variability

The spatial mismatch between the large-scale forcing datasets used to drive the model and the field measurements can explain part of the discrepancies between the simulations and the measurements. Due to the low topographic variability of the area, the climate observations of the Avignon site are representative of the area covered by the reanalysis grid. This particularly holds true for radiation but larger variability can be found for precipitation. The large-scale vegetation and soil data cannot exactly match the local ones but their evaluation at local scale brings insight on their representativeness of typical cropland and soil of the studied region.

The outcomes of this work show that the challenge for the spatial integration of a land surface model over Mediterranean cropland mainly concern the representation of the spatial variability in rainfall, irrigation, vegetation dynamic and soil hydrodynamic properties at the regional scale. Regarding rainfall, we showed that it is the main climate driver of the errors in yearly ET. It is thus of paramount importance to improve the description of its spatiotemporal heterogeneity to improve the simulation of water balance at regional scale. While the SAFRAN rainfall is probably the most accurate and precise reanalysis dataset over France, Zhao et al. (2012) showed that its spatial resolution may not be fine enough to resolve rainfall spatial heterogeneity. This particularly holds true for Mediterranean regions where rainfalls are governed more by local convective elements and mesoscale convection than by large-scale well-resolved dynamical processes. The impact of the lack of irrigation on ET reported in this work provides an indication of the errors that could be generated by the use of inaccurate rainfall forcing over large areas. High resolution rainfall datasets derived from the combination of terrestrial rainfall radar data, in situ observations and atmospheric models need to be developed to resolve rainfall spatial heterogeneity at regional scale. Regarding irrigation, more accurate description of the variability of irrigation practices need to be incorporated in LSMs (Ozdogan et al., 2010; Olioso et al., 2013). Regarding the soil parameters, the pedotransfer functions need to be improved to better resolve the spatial variability of soil properties. Inverse modelling strategy could be developed to retrieve the soil parameters and the associated uncertainties (Scharnagl et al., 2011). Regarding vegetation dynamic, the use of satellite observations with finer spatial and temporal resolution (e.g. next SENTINEL-2 satellite) should provide finer description of the LAI cycle of crops.

GMDD
8, 2053–2100, 2015

8 Summary

The present study focuses on the errors in the large-scale forcing variables used to describe the climate (rainfall, downwelling shortwave and longwave radiations), the irrigation, the soil texture and the vegetation dynamic (Leaf Area Index, LAI). It aims at assessing their impacts on the evapotranspiration (ET) simulated from the ISBA-A-gs land surface model over a 12 year Mediterranean crop succession. We evaluate the forcing datasets used in the standard implementation of ISBA over France where the model is driven by the SAFRAN high spatial resolution atmospheric reanalysis, the LAI cycles derived from the Ecoclimap-II land surface parameter database and the soil texture derived from the French soil database. For climate, additional datasets used to drive the model at the continental scale are tested which includes the ERA-Interim low spatial resolution reanalysis, the GPCC rainfall dataset and the downwelling shortwave radiation derived from the MSG satellite. The methodology consists in comparing the simulation achieved using large-scale forcing dataset and the simulation achieved using local observations for each forcing variable. The performances of each simulation are quantified against ET measurements. The relative impact of the forcing variables on ET are compared with each other and with the modeling uncertainties triggered by errors in soil parameters. The main outcomes of this work are:

- LAI and the lack of irrigation generate the largest mean deviations in ET between the large-scale and the local-scale simulations (equivalent to 24 and 19 months of ET over 12 yr). The climate induces smaller mean deviations (equivalent to 7–8 months of ET over 12 yr). The impact of the errors in the forcing variables is smaller than the impact triggered by errors in the soil hydrodynamic parameters.

- The absence of irrigation which represents 18 % of cumulative rainfall over 12 years induces a deficit in ET of 14 %. It generates much larger variations in incoming water for the model than the differences in rainfall between the reanalysis datasets. Its simulation by the model was tested and provide inaccurate irrigation amount and timing for the crops under study.

GMDD
8, 2053–2100, 2015

– ET simulated with the Ecoclimap-II LAI climatology is overestimated by 18 % over 12 years. This is related to the overestimation of the mean LAI over the crop cycle which reveals inaccurate representation of Mediterranean crop cycles.

– Compared to the SAFRAN climate, the use of the ERA-I reanalysis, the GPCC rainfall and the satellite shortwave radiation have little influence on the ET simulation performances. The error in yearly ET is mainly driven by the errors in yearly rainfall and to a less extent by radiations. SAFRAN and MSG shortwave radiation estimates show similar negative biases (−9 and −11 $W m^{-2}$). The ERA-I bias in shortwave radiation is 4 times smaller at daily time scale. Both SAFRAN and ERA-I underestimates longwave radiation by −12 and −16 $W m^{-2}$, respectively. The biases in shortwave and longwave radiations show larger inter-annual variation for SAFRAN than for ERA-I. Regarding rainfall, SAFRAN and ERA-I/GPCC are slightly biased at daily and longer time scales (1 and 0.5 % of the mean rainfall measurement). The SAFRAN rainfall estimates are more precise due to the use of the in situ daily rainfall measurements of the Avignon site in the reanalysis. ERA-I/GPCC shows large inter-annual variability in yearly rainfall error which can reach up to 100 mm.

References

Anquetin, S., Braud, I., Vannier, O., Viallet, P., Boudevillain, B., Creutin, J.-D., and Manus, C.: Sensitivity of the hydrological response to the variability of rainfall fields and soils for the Gard 2002 flash-flood event, J. Hydrol., 394, 134–147, 2010.

Avissar, R. and Pielke, R. A.: A parameterization of heterogeneous land surfaces for atmospheric numerical models and its impact on regional meteorology, Mon. Weather Rev., 117, 2113–2136, 1989.

Barbu, A. L., Calvet, J.-C., Mahfouf, J.-F., and Lafont, S.: Integrating ASCAT surface soil moisture and GEOV1 leaf area index into the SURFEX modelling platform: a land data assimilation application over France, Hydrol. Earth Syst. Sci., 18, 173–192, doi:10.5194/hess-18-173-2014, 2014.

Baroni, G., Facchi, A., Gandolfi, C., Ortuani, B., Horeschi, D., and van Dam, J. C.: Uncertainty in the determination of soil hydraulic parameters and its influence on the performance of two hydrological models of different complexity, Hydrol. Earth Syst. Sci. 14, 251–270, 2010.
Braud I., Dantas-Antonio, A. C., and Vauclin, M.: A stochastic approach to studying the influence of the spatial variability of soil hydraulic properties on surface fluxes, temperature and humidity, J. Hydrol., 165, 283–310, 1995.
Beziat, P., Ceschia, E., and Dedieu, G.: Carbon balance of a three crop succession over two cropland sites in South West France, Agr. Forest Meteorol., 149, 1628–1645, 2009.
Bosilovich, M.: Regional climate and variability of nasa merra and recent reanalyses: U.S. summertime precipitation and temperature, J. Appl. Meteorol. Clim., 52, 1939–1951, 2013.
Bosilovich, M., Kennedy, J., Dee, D., Allan, R., and O'Neill A.: On the reprocessing and reanalysis of observations for climate, in: Climate Science for Serving Society: Research, Modeling and Prediction Priorities, edited by: Asrar, G. R. and Hurrell, J. W., Springer, the Netherlands, 51–71, 2013.
Calvet, J.-C., Noilhan, J., Roujean, J.-L., Bessemoulin, P., Cabelguenne, M., Olioso, A., and Wigneron, J.-P.: An interactive vegetation SVAT model tested against data from six contrasting sites, Agr. Forest Meteorol., 92, 73–95,1998.
Calvet, J.: Investigating soil and atmospheric plant water stress using physiological and micrometeorological data, Agr. Forest Meteorol., 103, 229–247, 2000.
Calvet, J.-C., Gibelin, A.-L., Roujean, J.-L., Martin, E., Moigne, P. L., Douville, H., and Noilhan, J.: Past and future scenarios of the effect of carbon dioxide on plant growth and transpiration for three vegetation types of southwestern France, Atmos. Chem. Phys., 8, 397–406, 2008,
http://www.atmos-chem-phys.net/8/397/2008/.
Calvet, J.-C., Lafont, S., Cloppet, E., Souverain, F., Badeau, V., and Le Bas, C.: Use of agricultural statistics to verify the interannual variability in land surface models: a case study over France with ISBA-A-gs, Geosci. Model Dev., 5, 37–54, 2012.
Carrer, D., S. Lafont, J. L. Roujean, J. C. Calvet, C. Meurey, Le Moigne, P., and Trigo, I.: Incoming solar and infrared radiation derived from METEOSAT: impact on the modelled land water and energy budget over France, J. Hydrometeorol., 13, 504–520, 2012.
Clapp, R. and Hornberger, G.: Empirical equations for some soil hydraulic properties, Water Resour. Res., 14, 601–604, 1978.

Courault, D., Olioso, A., Lagouarde, J.-P., Monestiez, P., and Allard, D.: Influence des cultures sur les variables climatiques, in: Organisation spatiale des activités agricoles et processus environnementaux, edited by: Monestiez, P., Lardon, S., Seguin, B., Collection Science Update, INRA Editions, Paris, 303–320, 2004.

Decharme B., and Douville, H.: Uncertainties in the GSWP-2 precipitation forcing and their impacts on regional and global hydrological simulations, Clim. Dynam., 27, 695–713, doi:10.1007/s00382-006-0160-6, 2006.

de Rosnay, P., Polcher, J., Laval, K., and Sabre, M.: Integrated parameterization of irrigation in the land surface model ORCHIDE E, Validation over Indian Peninsula, Geophys. Res. Lett., 30, 1986, doi:10.1029/2003gl018024, 1986.

Decker, M., Brunke, M. A., Wang, Z., Sakaguchi, K., Zeng, X., and Bosilovich, M. G.: Evaluation of the reanalysis products from GSFC, NCEP, and ECMWF using flux tower observations, J. Climate, 25, 1916–1944, 2012.

Déqué, M., Dreveton C., Braun, A., and Cariolle, D.: The ARPEGE/IFS atmosphere model: a contribution to the French community climate modelling, Clim. Dynam. 10, 249–266, doi:10.1007/BF00208992, 1994.

Duveiller, G., Weiss, M., Baret, F., and Defourny, P.: Retrieving wheat Green Area Index during the growing season from optical time series measurements based on neural network radiative transfer inversion, Remote Sens. Environ., 115, 887–896, 2011.

Espino, A., Mallants, D., Vanclooster, M., and Feyen, J.: Cautionarynotes on the use of pedotransfer functions for estimating soil hydraulic properties, Agr. Water Manage., 29, 235–253, 1996.

Faroux, S., Kaptué Tchuenté, A. T., Roujean, J.-L., Masson, V., Martin, E., and Le Moigne, P.: Ecoclimap-II/Europe: a twofold database of ecosystems and surface parameters at 1 km resolution based on satellite information for use in land surface, meteorological and climate models, Geosci. Model Dev., 6, 563–582, doi:10.5194/gmd-6-563-2013, 2013.

Foken, T., Göckede, M., Mauder, M., Mahrt, L., Amiro, B., and Munger, W.: Post-field data quality control, in: Handbook of Micrometeorology, edited by: Lee, X., Massman, W. and Law, B. E., Kluwer Academic Publishers, Dordrecht, the Netherlands, 181–208, 2004.

Foken, T., Göcked, M., Mauder, M., Mahrt, L., Amiro, B., and Munger, W.: Post-field data quality control, in: Handbook of Micrometeorology, edited by: Lee, X., Massman, W., and Law, B. E., Kluwer Academic Publishers, Dordrecht, the Netherlands, 181–208, 2004.

Garrigues, S., Lacaze, R., Baret, F., Morisette, J. T., Weiss, M., Nickeson, J., Fernandes, R., Plummer, S., Shabanov, N. V., Myneni, R., Knyazikhin, Y., and Yang, W.: Validation and intercomparison of global Leaf Area Index product derived from remote sensing data, J. Geophys. Res., 113, G02028, doi:10.1029/2007JG000635, 2008.

Garrigues, S., Olioso, A., Calvet, J.-C., Martin, E., Lafont, S., Moulin, S., Chanzy, A., Marloie, O., Desfonds, V., Bertrand, N., and Renard, D.: Evaluation of land surface model simulations of evapotranspiration over a 12 year crop succession: impact of the soil hydraulic properties, Hydrol. Earth Syst. Sci. Discuss., 11, 11687–11733, doi:10.5194/hessd-11-11687-2014, 2014.

Ge, J., Qi, J., Lofgren, B. M., Moore, N., Torbick, N., and Olson, J. M.: Impacts of land use/cover classification accuracy on regional climate simulations, J. Geophys. Res., 112, D05107, doi:10.1029/2006JD007404, 2007.

Geiger, B., Meurey, C., Lajas, D., Franchisteguy, L., Carrer, D., and Roujean, J.-L.: Near real-time provision of downwelling shortwave radiation estimates derived from satellite observations, Meteor. Appl., 15, 411–420, 2008.

Gibelin, A.-L., Calvet, J.-C., Roujean, J.-L., Jarlan, L., and Los, S. O.: Ability of the land surface model ISBA-A-gs to simulate leaf area index at the global scale: comparison with satellites products, J. Geophys. Res., 111, 1–16, 2006.

Habets, F., Boone, A., Champeaux, J. L., Etchevers, P., Franchisteguy, L., Leblois, E., Ledoux, E., Moigne, P. L., Martin, E., Morel, S., Noilhan, J., and Viennot, P.: The SAFRAN-ISBA-MODCOU hydrometeorological model applied over France, J. Geophys. Res., 113, 1–18, 2008.

Hendricks Franssen, H. J., Stöckli, R., Lehner, I., Rotenberg, E., and Seneviratne, S. I.: Energy balance closure of eddy-covariance data: A multisite analysis for European FLUXNET stations, Agr. Forest Meteorol., 150, 1553–1567, 2010.

Ingwersen, J., Steffens, K., Högy, P., Zhunusbayeva, D., Poltoradnev, M., Gäbler, R., Wizemann, H., Fangmeier, A., Wulfmeyer, V., and Streck, T.: Comparison of Noah simulations with eddy covariance and soil water measurements at a winter wheat stand, Agr. Forest Meteorol., 151, 345–355, 2011.

King, D., Lebas, C., Jamagne, M., Hardy, R., and Daroussin, J: Base de données géographiques des sols de France a l'échelle 1/1 000 000 (Geographical Soil Database for France at a scale of 1/1 000 000), Technical report, 100 pp., Institut National de Recherches

Agronomiques (INRA), Orleans, France, available at: http://www.gissol.fr/programme/bdgsf/bdgsf.php, 1995.
Lafont, S., Zhao, Y., Calvet, J.-C., Peylin, P., Ciais, P., Maignan, F., and Weiss, M.: Modelling LAI, surface water and carbon fluxes at high-resolution over France: comparison of ISBA-A-gs and ORCHIDEE, Biogeosciences, 9, 439–456, doi:10.5194/bg-9-439-2012, 2012.
Leng, G., Huang, M., Tang, Q., Sacks, W. J., Lei, H., and Leung, L. R.: Modeling the effects of irrigation on land surface fluxes and states over the conterminous United States: Sensitivity to input data and model parameters, J. Geophys. Res. Atmos. 118, 9789–9803, doi:10.1002/jgrd.50792, 2013.
Maggioni, V., Anagnostou, E. N., and Reichle, R. H.: The impact of model and rainfall forcing errors on characterizing soil moisture uncertainty in land surface modeling, Hydrol. Earth Syst. Sci. 16, 3499–3515, 2012.
Mahfouf, J.-F. and Noilhan, J.: Inclusion of gravitational drainage in a land surface scheme based on the force-restore method, J. Appl. Meteorol., 35, 987–992, 1996.
Masson, V, Champeaux, J.-L., Chauvin, F., Meriguet, C., and Lacaze, R.: A global database of land surface parameters at 1 km resolution in meteorological and climate models, J. Climate, 16, 1261–1282, 2003.
Masson, V., Le Moigne, P., Martin, E., Faroux, S., Alias, A., Alkama, R., Belamari, S., Barbu, A., Boone, A., Bouyssel, F., Brousseau, P., Brun, E., Calvet, J.-C., Carrer, D., Decharme, B., Delire, C., Donier, S., Essaouini, K., Gibelin, A.-L., Giordani, H., Habets, F., Jidane, M., Kerdraon, G., Kourzeneva, E., Lafaysse, M., Lafont, S., Lebeaupin Brossier, C., Lemonsu, A., Mahfouf, J.-F., Marguinaud, P., Mokhtari, M., Morin, S., Pigeon, G., Salgado, R., Seity, Y., Taillefer, F., Tanguy, G., Tulet, P., Vincendon, B., Vionnet, V., and Voldoire, A.: The SURFEXv7.2 land and ocean surface platform for coupled or offline simulation of earth surface variables and fluxes, Geosci. Model Dev., 6, 929–960, doi:10.5194/gmd-6-929-2013, 2013.
Mauder, M., Cuntz, M., Drüe, C., Graf, A., Rebmann, C., Schmid, H. P., Schmidt, M., and Steinbrecher, R.: A strategy for quality and uncertainty assessment of long-term eddy-covariance measurements, Agr. Forest Meteorol., 169, 122–135, 2013.
Miralles, D. G., De Jeu, R. A. M., Gash, J. H., Holmes, T. R. H., and Dolman, A. J.: Magnitude and variability of land evaporation and its components at the global scale, Hydrol. Earth Syst. Sci., 15, 967–981, doi:10.5194/hess-15-967-2011, 2011.
Moureaux, C., Ceschia, E., Arriga, N., Beziat, P., Eugster., Kutsch, W. L., and Pattey, E.: Eddy Covariance Measurements over Crops, in: Eddy Covariance: A Practical Guide to Measure-

ment and Data Analysis, edited by: Aubinet, M., Vesala, T., and Papale, D., Springer, Dordrecht, the Netherlands, 319–332, 2012.

Nash, J. E. and Sutcliffe, J. V.:. River flow forecasting through conceptual models, part I, a discussion of principles, J. Hydrol., 10, 282–290, 1970.

Noilhan, J. and Planton, S.: A simple parameterization of land surface processes for meteorological models, Mon. Weather Rev., 117, 536–549, 1989.

Noilhan, J. and Lacarrère, P.: GCM grid-scale evaporation from mesocale modeling, J. Climate, 8, 206–223, 1995.

Noilhan, J. and Mahfouf, J.-F.: The ISBA land surface parameterisation scheme, Global Planet. Change, 13, 145–159, 1996.

Noilhan, J., Donier, S., Sarrat, C., and Moigne, P. L.: Regional-scale evaluation of a land surface scheme from atmospheric boundary layer observations, J. Geophys. Res., 116, 1–17, 2011.

Olioso, A., Inoue, Y., Ortega-FARIAS, S., Demarty, J., Wigneron, J.-P., Braud, I., Jacob, F., Lecharpentier, P., Ottlé, C., Calvet, J.-C., and Brisson, N.: Future directions for advanced evapotranspiration modeling: assimilation of remote sensing data into crop simulation models and SVAT models, Irrig. Drain., 19, 377–412, 2005.

Olioso, A., Lecerf, R., Baillieux, A., Chanzy, A., Ruget, F., Banton, O., Lecharpentier, P., Trolard, F., and Cognard-Plancq, A.-L.: Modelling of drainage and hay production over the Crau aquifer for analysing impact of global change on aquifer recharge, Proc. Env. Sci., 19, 69–700, 2013.

Ozdogan, M., Rodell, M., Beaudoing, H. K., and Toll, D. L.: Simulating the effects of irrigation over the United States in a land surface model based on satellite-derived agricultural data, J. Hydrometeorol. 11, 171–184, doi:10.1175/2009JHM1116.1, 2010.

Quintana-Seguí, P., Le Moigne, P., Durand, Y., Martin, E., Habets, F., Baillon, M., Canellas, C., Franchisteguy, L., and Morel, S.: Analysis of near-surface atmospheric variables: validation of the SAFRAN analysis over France, J. Appl. Meteorol. Clim., 47, 92–107, 2008.

Rebmann, C., Kolle., O., Heinesch, B., Queck, R., Ibrom, A., and Aubinet, M.: Data acquisition and flux calculation, in: Eddy Covariance: A Practical Guide to Measurement and Data Analysis, edited by: Aubinet, M., Vesala, T., and Papale, D., Springer, Dordrecht, the Netherlands, 59–84, 2012.

Ritter, B. and Geleyn J.-F.: A comprehensive radiation scheme for numerical weather prediction models with potential applications in climate simulations, Mon. Weather Rev., 120, 303–325, 1992.

Scharnagl, B., Vrugt, J. A., Vereecken, H., and Herbst, M.: Inverse modelling of in situ soil water dynamics: investigating the effect of different prior distributions of the soil hydraulic parameters, Hydrol. Earth Syst. Sci., 15, 3043–3059, doi:10.5194/hess-15-3043-2011, 2011.
Schneider, U., Becker, A., Finger, P., Meyer-Christoffer, A., Rudolf, B., and Ziese, M.: GPCC Full Data Reanalysis Version 6.0 at 0.5°: Monthly Land–Surface Precipitation from Rain-Gauges built on GTS-based and Historic Data, Global Precipitation Climatology Centre (GPCC, http://gpcc.dwd.de/) at Deutscher Wetterdienst, 2011.
Simmons, A. J., Willett, K. M., Jones, P. D., Thorne, P. W., and Dee, D. P.: Low-frequency variations in surface atmospheric humidity, temperature and precipitation: inferences from reanalyses and monthly gridded observational data sets, J. Geophys. Res., 115, D01110, doi:10.1029/2009JD012442, 2010.
Szczypta, C., Calvet, J.-C., Albergel, C., Balsamo, G., Boussetta, S., Carrer, D., Lafont, S., and Meurey, C.: Verification of the new ECMWF ERA-Interim reanalysis over France, Hydrol. Earth Syst. Sci., 15, 647–666, doi:10.5194/hess-15-647-2011, 2011.
Teuling, A. J., Hirschi, M., Ohmura, A., Wild, M., Reichstein, M., Ciais, P., Buchmann, N., Ammann, C., Montagnani, L., Richardson, A. D., Wohlfahrt, G., and Seneviratne, S. I.: A regional perspective on trends in continental evaporation, Geophys. Res. Lett., 36, published online, doi:10.1029/2008GL036584, 2009.
Vidal, J.-P., Martin, E., Franchistéguy, L., Habets, F., Soubeyroux, J.-M., Blanchard, M., and Baillon, M.: Multilevel and multiscale drought reanalysis over France with the Safran-Isba-Modcou hydrometeorological suite, Hydrol. Earth Syst. Sci., 14, 459–478, doi:10.5194/hess-14-459-2010, 2010a.
Vidal, J.-P., Martin, E., Franchistéguy, L., Baillon, M., and Soubeyroux, J.-M.: A 50 year high-resolution atmospheric reanalysis over France with the Safran system, Int. J. Climatol., 30, 1627–1644, 2010b.
Wang, A. and Zeng, X.: Evaluation of multireanalysis products with in situ observations over the Tibetan Plateau, J. Geophys. Res., 117, D05102, doi:10.1029/2011JD016553, 2012.
Wilson, K., Goldstein, A., Falge, E., Aubinet, M., Baldocchi, D., Berbigier, P., Bernhofer, C., Ceulemans, R., Dolman, H., Field, C., Grelle, A., Ibrom, A., Law, B. E., Kowalski, A., Meyers, T., Moncrieff, J., Monson, R., Oechel, W., Tenhunen, J., Valentini, R., and Verma, S.: Energy balance closure at FLUXNET sites, Agr. Forest Meteorol., 113, 223–243, 2002.
Zhao, Y., Ciais, P., Peylin, P., Viovy, N., Longdoz, B., Bonnefond, J. M., Rambal, S., Klumpp, K., Olioso, A., Cellier, P., Maignan, F., Eglin, T., and Calvet, J. C.: How errors on meteorologi-

cal variables impact simulated ecosystem fluxes: a case study for six French sites, Biogeosciences, 9, 2537–2564, doi:10.5194/bg-9-2537-2012, 2012.
Zhao, T., Guo, W., and Fu, C.: Calibrating and evaluating reanalysis surface temperature error by topographic correction, J. Climate, 21, 1440–1446, 2008.

GMDD
8, 2053–2100, 2015

Table 1. Definition of symbols and acronyms.

BIAS	Bias computed as the mean deviation between the simulated variable and the measured variable. It quantifies the accuracy of the simulation.
BS	Bare soil
C3	C3 type of crop
C4	C4 type of crop
d_2	Rooting depth (m)
ERA-I	ERA-Interim reanalysis climate dataset (spatial resolution of 0.5° and time step of 3 h)
ERA-I/GPCC	ERA-I climate where rainfall was corrected using the GPCC rainfall dataset
GPCC	Global Precipitation Climatology Centre dataset (version 6, Schneider et al., 2011) which gives monthly quality-controlled precipitation totals.
Ecoclimap-II	Land surface parameter database (spatial resolution of 1 km) used to run the SURFEX/ISBA model at global scale (Faroux et al., 2013).
ET	Evapotranspiration (given in cumulative value in mm at daily or multi-year time scales)
f_{clay}	Clay fraction
f_{sand}	Sand fraction
FSDB	French Soil DataBase (King et al., 1995) which provides soil texture over the SAFRAN grid at a spatial resolution of 8 km.
ISBA	Interactions between Soil, Biosphere, and Atmosphere (ISBA) Land surface model.
ISBA-A-gs	A-gs version of ISBA. A-gs indicates that ISBA includes a coupled stomatal conductance-photosynthesis scheme.
LAI	Leaf Area Index ($m^2 m^{-2}$)
LE	Latent heat flux ($W m^{-2}$)
LSM	Land Surface Model
MaxAWC	Maximum Available Water Content. It represents the maximum water stock available for the crop's growth.
MD	Mean deviation
MSG	MeteoSat Second Generation satellite. We used the downwelling shortwave radiation derived from MSG observations.
NI	Nash Index
NR	Net Radiation
r	Correlation coefficient
RMSD	Root Mean Square of Differences (between two simulations)
RMSE	Root Mean Square Error (between a simulated variable and its measurement)
SAFRAN	Système d'Analyse Fournissant des Renseignements Atmosphériques à la Neige' Analysis system providing data for snow model. The SAFRAN reanalysis covers France with a spatial resolution of 8 km and at hourly time step.
SD	Standard deviation
SDD	SD of the differences
SEVIRI	Spinning Enhanced Visible and Infrared Imager instrument on board the MeteoSat Second Generation Satellite
SURFEX	"Surface externalisée" in French. SURFEX is an externalized land and ocean surface platform that describes the surface fluxes and the evolution of four types of surface: nature, town, inland water and ocean. ISBA is the land surface model used for nature surfaces.
SWdown	Downwelling shortwave radaition
LWdown	Downwelling longwave radaition
w_{fc}	volumetric soil moisture at field capacity ($m^3 m^{-3}$)
w_{sat}	volumetric soil moisture at saturation ($m^3 m^{-3}$)
w_{wp}	volumetric soil moisture at wilting point ($m^3 m^{-3}$)

GMDD
8, 2053–2100, 2015

Table 2. 2001–2012 crop succession. T and Rain are the mean temperature and cumulative precipitation, respectively, over the crop cycle.

Year	Crop	Sowing date	Harvest date	Rain (mm)	T (°C)	Irrigation (mm)	Simulated Irrigation (mm)
2001	Maize	25 April 2001	28 September 2001	232.0	20.7	375	300
2002	Wheat	23 October 2001	2 July 2002	399.0	11.6	0	na
2003	Sunflower[1]	16 April 2003	26 May 2003	68.0	17.1	40	120
2003	Sunflower	2 June 2003	19 September 2003	68.5	24.8	225	540
2004	Wheat	7 November 2003	28 June 2004	422.0	11.2	0	na
2005	Peas	13 January 2005	22 June 2005	203.5	11.9	100	330
2006	Wheat	27 October 2005	27 June 2006	256.0	10.7	20	na
2007	Sorghum	10 May 2007	16 October 2007	168.5	20.6	80	300
2008	Wheat	13 November 2007	1 July 2008	502.5	11.7	20	na
2009	Maize[1]	23 April 2009	15 June 2009	110.5	19.2	80	0
2009	Sorghum	25 June 2009	22 September 2009	89.0	23.6	245	300
2010	Wheat	19 November 2009	13 July 2010	446.5	11.6	0	na
2011	Sorghum	22 April 2011	22 September 2011	268.5	21.4	60	180
2012	Wheat	19 October 2011	25 June 2012	437.0	12.0	0	na

[1] These crops were interrupted and replaced by a new one.

GMDD
8, 2053–2100, 2015

Table 3. Characteristics of the simulations. FSDB stands for the French Soil DataBase used for the large-scale soil texture. C3 and C4 correspond to the SURFEX crop patches and BS is the bare soil patch. f_{sand}, f_{clay} are the fractions of sand and clay. d_2 is the depth of the root zone. w_{fc}, w_{wp} and w_{sat} are the volumetric soil moisture at field capacity, wilting point and saturation. MaxAWC represents the maximum water stock available for the crop's growth. It is computed as d_2*(w_{fc}-w_{wp}). Cells with gray background indicate the local values of the forcing variables or soil parameters. S_{CTL} is the control simulation, based on local observations for the climate, the irrigation, the soil texture, the vegetation dynamic and the soil hydrodynamic parameters.

		Simulations S_{SAF}	S_{ERA}	S_{GPCC}	S_{MSG}	S_{clim}	$S_{clim, irri}$	$S_{clim, irri, text}$	$S_{clim, irri, text, veg}$	S_{CTL}
Forcing variables	CLIMATE									
	Rainfall	**SAFRAN**	**ERA-I/GPCC**	**ERA-I/GPCC**	**SAFRAN**	Local	Local	Local	Local	Local
	Shortwave radiation	**SAFRAN**	**ERA-I**	**SAFRAN**	**MSG**	Local	Local	Local	Local	Local
	Other climate variables	**SAFRAN**	**ERA-I**	**SAFRAN**	**SAFRAN**	Local	Local	Local	Local	Local
	SURFACE									
	Irrigation	**NO**	**NO**	**NO**	**NO**	**NO**	Local	Local	Local	Local
	Texture	**FSDB**	**FSDB**	**FSDB**	**FSDB**	**FSDB**	**FSDB**	Local	Local	Local
	f_{clay}; f_{sand}	**0.18; 0.2**	**0.18; 0.2**	**0.18; 0.2**	**0.18; 0.2**	**0.18; 0.2**	**0.18; 0.2**	0.33; 0.14	0.33; 0.14	0.33; 0.14
	LAI	**Ecoclimap**	**Ecoclimap**	**Ecoclimap**	**Ecoclimap**	**Ecoclimap**	**Ecoclimap**	**Ecoclimap**	Local	Local
	Vegetation height	**Ecoclimap**	**Ecoclimap**	**Ecoclimap**	**Ecoclimap**	**Ecoclimap**	**Ecoclimap**	**Ecoclimap**	Local	Local
Soil Parameters	Estimation method	ISBA pedotransfer function								In situ
	w_{sat} ($m^3 m^{-3}$)	0.473	0.473	0.473	0.473	0.473	0.473	0.479	0.479	0.390
	w_{fc} ($m^3 m^{-3}$)	0.245	0.245	0.245	0.245	0.245	0.245	0.303	0.3	0.310
	w_{wp} ($m^3 m^{-3}$)	0.158	0.158	0.158	0.158	0.158	0.158	0.214	0.214	0.184
	MaxAWC C3, C4 (mm)	109, 131	109, 131	109, 131	109, 131	109, 131	109, 131	111, 134	111, 134	189, 189
	d_2 C3, C4, BS (m)	1.25, 1.5, 0.5	1.25, 1.5, 0.5	1.25, 1.5, 0.5	1.25, 1.5, 0.5	1.25, 1.5, 0.5	1.25, 1.5, 0.5	1.25, 1.5, 0.5	1.25, 1.5, 0.5	1.5, 1.5, 1.5

Table 4. Influence of the large-scale forcing variables on the simulated evapotranspiration (ET) at half-hourly (LE is used), daily and 12 yr time scales. The simulation achieved with large-scale forcing is compared with the simulation performed with local forcing for distinct drivers. The last row concerns the impact of using in situ soil parameters instead of the ISBA pedotransfer function estimates. The comparison metrics were computed over the 25 April 2001–26 June 2012 period. r is the correlation coefficient. RMSD is the root mean square of the differences, MD is the mean difference (for Y vs. X, MD is computed as Y-X.), SDD is the SD of the differences. In the last column, MD in cumulative ET over 12 yr is given in absolute value and in percentage of the 12 yr cumulative ET simulated using the local forcing. The latter is translated in equivalent number of months of ET.

		Half-hourly LE ($W\,m^{-2}$)				Daily ET ($mm\,day^{-1}$)				12 yr cumulative ET		
Tests	Simulations	r	RMSD	MD	SDD	r	RMSD	MD	SDD	MD (mm)	MD (%)	MD (months of ET)
Climate: SAFRAN vs. local climate	$S_{SAF} - S_{clim}$	0.87	38.3	−2.4	38.3	0.88	0.66	−0.08	0.65	−343	5.9	7.9
Climate: ERA-I/GPCC vs. local climate	$S_{ERA} - S_{clim}$	0.76	51.8	−1.9	51.7	0.82	0.79	−0.07	0.79	−286	4.9	6.6
Rainfall: SAFRAN climate and ERA-I/GPCC rainfall vs. local climate	$S_{GPCC} - S_{clim}$	0.82	44.9	−2.5	44.8	0.81	0.82	−0.09	0.82	−355	6.1	8.1
Shortwave radiation: SAFRAN climate and MSG shortwave radiation vs. local climate	$S_{MSG} - S_{clim}$	0.88	38.9	−2.6	38.8	0.89	0.63	−0.09	0.62	−367	6.3	8.4
Irrigation: No irrigation vs. local irrigation	$S_{clim} - S_{clim,\,irri}$	0.89	43.0	−6.7	42.5	0.85	0.94	−0.24	0.91	−973	14.3	19.1
Soil texture: French database vs. local soil texture	$S_{clim,\,irri} - S_{clim,\,irri,\,text}$	1.00	9.0	−1.1	9.0	1.00	0.14	−0.04	0.13	−156	2.2	3.0
Vegetation dynamic: Ecoclimap-II vs. local LAI	$S_{clim,\,irri,\,text} - S_{clim,\,irri,\,text,\,veg}$	0.87	47.5	7.4	46.9	0.84	0.99	0.26	0.96	1063	18.0	24.1
Soil hydrodynamic parameters: Pedotransfer vs. in situ estimates	$S_{clim,\,irri,\,text,\,veg} - S_{CTL}$	0.92	38.6	−10.3	37.2	0.92	0.79	−0.36	0.71	−1470	20.0	26.7

GMDD
8, 2053–2100, 2015
Impact of forcing variables on ISBA-A-gs simulation of ET
S. Garrigues et al.

Table 5. Performance scores of ET simulations evaluated against in situ eddy-covariance measurements. The metrics were computed over the 25 November 2003–26 June 2012 period for which the direct latent heat flux (LE) measurements were available. Daily ET was computed when 90 % of daytime measurements were valid for each day. The detailed characteristics of the simulations are provided in Table 3.

	LE ($W m^{-2}$)				Daily ET ($mm day^{-1}$)				12 year cumulative ET (mm)
Simulations	RMSE	BIAS	SDD	NI	RMSE	BIAS	SDD	NI	BIAS
S_{SAF}	57.1	−13.1	55.6	0.46	0.94	−0.22	0.92	0.40	−880 (23 %)
S_{ERA}	65.5	−14.1	64.0	0.29	0.98	−0.29	0.94	0.35	−954 (25 %)
S_{GPCC}	59.2	−13.1	57.8	0.42	0.97	−0.21	0.95	0.36	−882 (24 %)
S_{MSG}	60.7	−13.6	59.2	0.39	0.95	−0.24	0.92	0.39	−917 (24 %)
S_{clim}	55.6	−10.8	54.5	0.49	0.92	−0.21	0.89	0.42	−731 (19 %)
$S_{clim, irri}$	54.3	−5.5	54.0	0.51	0.89	−0.06	0.89	0.46	−369 (10 %)
$S_{clim, irri, text}$	53.1	−4.4	52.9	0.53	0.87	−0.04	0.87	0.48	−290 (8 %)
$S_{clim, irri, text, veg}$	53.8	−13.2	52.1	0.52	0.90	−0.27	0.86	0.45	−892 (24 %)
S_{CTL}	53.7	−0.6	53.7	0.52	0.84	0.07	0.84	0.52	−40 (1 %)

GMDD
8, 2053–2100, 2015

Table 6. Evaluation of SAFRAN and ERA-I/GPCC cumulative rainfall against measurements over the 2001–2012 period at 3 h, daily, 10 days, 30 days and yearly time scales. SDD and BIAS are given in absolute value (in mm) and in percentage of the mean in situ measurement.

	3 h			Daily			10 days			30 days			yearly		
Mean in situ meas. (mm)	0.22			1.74			17.36			51.83			657.10		
	r	**BIAS**	**SDD**	*r*	**BIAS**	**SDD**	*r*	**BIAS**	**SDD**	*r*	**BIAS**	**SDD**	*r*	**BIAS**	**SDD**
SAFRAN	0.53	0.00 (1 %)	1.46 (674 %)	0.97	0.02 (1 %)	1.57 (90 %)	0.98	0.21 (1 %)	4.48 (26 %)	0.99	0.61 (1 %)	7.03 (14 %)	0.99	8.22 (1 %)	20.14 (3 %)
ERA-I/GPCC	0.46	−0.14 (66 %)	1.57 (720 %)	0.73	0.01 (0.5 %)	4.69 (270 %)	0.84	0.09 (0.5 %)	14.31 (82 %)	0.90	0.28 (0.5 %)	21.89 (42 %)	0.95	4.45 (0.7 %)	60.00 (9.1 %)

GMDD
8, 2053–2100, 2015

Impact of forcing variables on ISBA-A-gs simulation of ET

S. Garrigues et al.

Table 7. Evaluation of SAFRAN, ERA-I and MSG downwelling shortwave radiation (SWdown), downwelling longwave radiation (LWdown) and simulated net radiation (NR) against measurements, over the 12 October 2004–25 June 2012 period, at 3 h and daily time steps. The SWdown performances of all the datasets were evaluated considering only the time steps with valid MSG SWdown, which represents 93 % of the period.

	3 h									Daily								
	SWdown ($W m^{-2}$)			LWdown ($W m^{-2}$)			NR ($W m^{-2}$)			SWdown ($W m^{-2}$)			LWdown ($W m^{-2}$)			NR ($W m^{-2}$)		
	r	BIAS	SDD	r	BIAS	SDD	r	BIAS	SDD	r	BIAS	SDD	r	BIAS	SDD	r	BIAS	SDD
SAFRAN	0.97	−9.5	65.8	0.79	−11.9	29.4	0.95	−4.5	55.4	0.95	−9.8	32.5	0.90	−11.9	19.2	0.86	−4.4	30.5
ERA-I	0.96	2.2	70.2	0.93	−16.1	17.4	0.87	4.8	87.5	0.96	2.1	28.4	0.97	−16.1	11.0	0.93	4.8	21.9
MSG	0.96	−11.2	67.6	NA	NA	NA	0.95	−3.7	54.4	0.95	−11.6	30.2	NA	NA	NA	0.90	−3.7	26.6

GMDD
8, 2053–2100, 2015

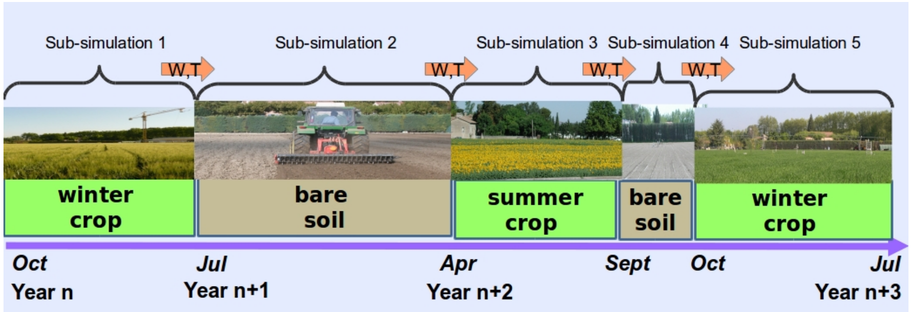

Figure 1. Illustration of the typical succession of winter and summer crop over the Avignon site. To represent the 12 yr crop succession in the simulation, the 12 year period is split into sub-simulation periods corresponding to crop and inter-crop periods. The simulation was initialized once on 25 April 2001 using the in situ soil temperature and soil moisture measurements. To ensure the continuity between 2 contiguous sub-simulations, each sub-simulation was initialized using the simulated soil moisture (W) and soil temperature (T) of the last time step of the previous sub-simulation.

GMDD
8, 2053–2100, 2015

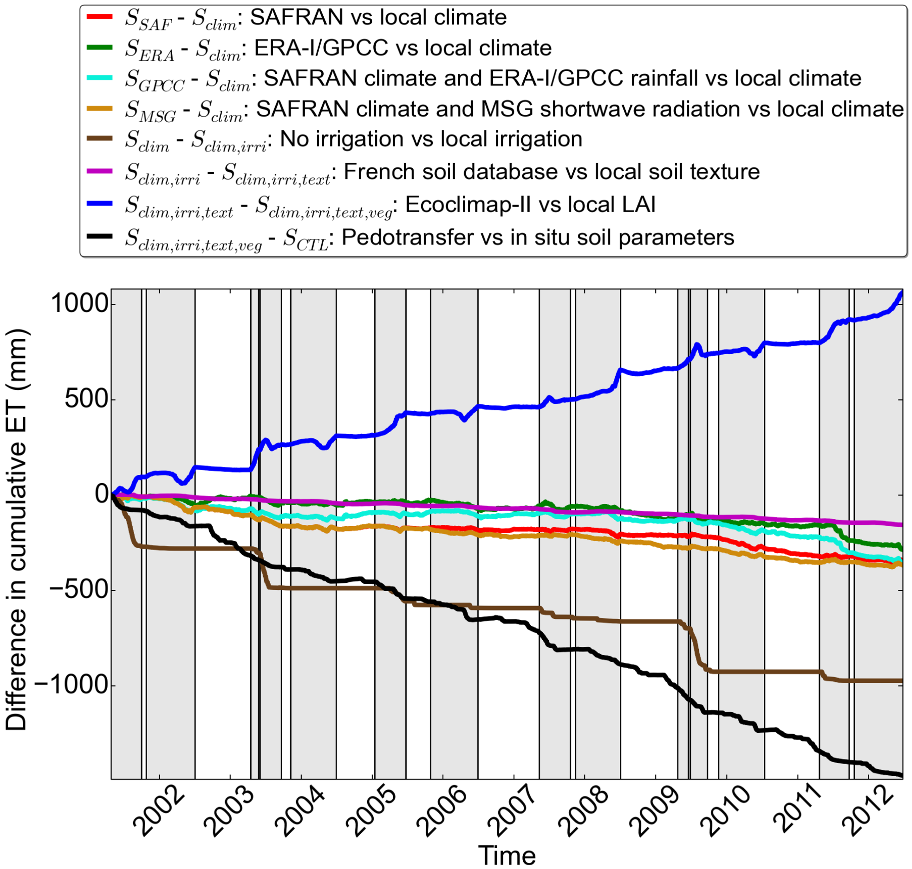

Figure 2. Differences in cumulative ET between the simulation achieved with large-scale forcing datasets and the simulation based on local observations for each tested forcing variable. The detailed characteristics of the simulations are given in Table 3. Crop periods and inter-crop periods are represented by grey background and white background, respectively.

GMDD
8, 2053–2100, 2015

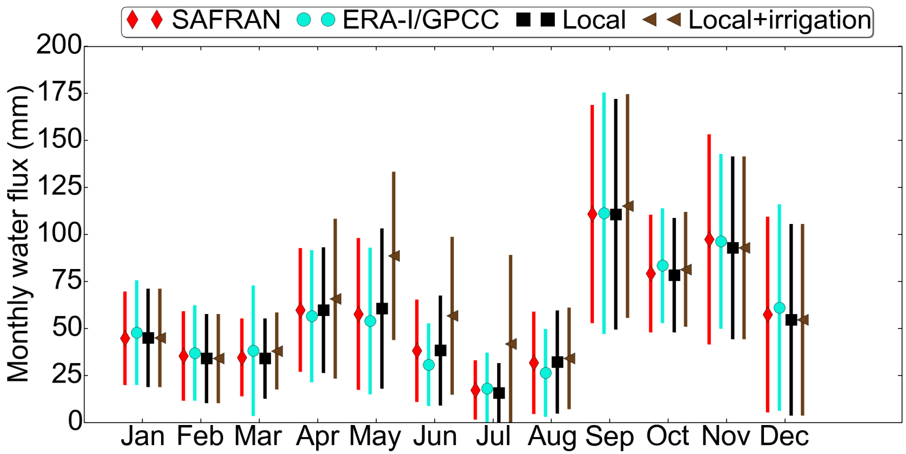

Figure 3. Comparison of SAFRAN, ERA-I/GPCC and local mean monthly rainfall. Irrigation amount added to the local rainfall is also presented. The vertical bars represent the inter-annual variability (± one SD).

GMDD

8, 2053–2100, 2015

Impact of forcing variables on ISBA-A-gs simulation of ET

S. Garrigues et al.

Title Page
Abstract Introduction
Conclusions References
Tables Figures
◂ ▸
Back Close
Full Screen / Esc
Printer-friendly Version
Interactive Discussion

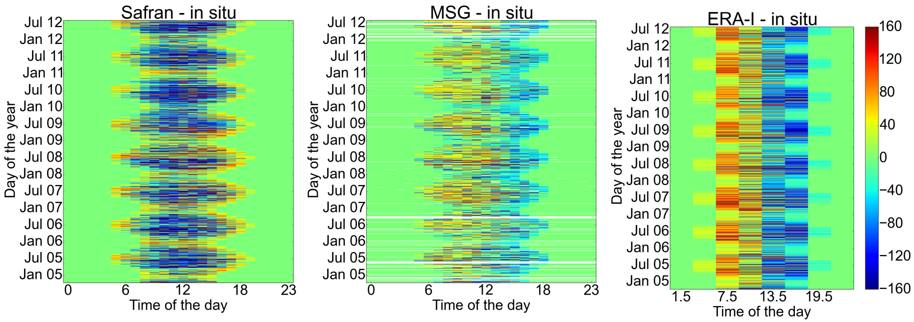

Figure 4. Comparison of SAFRAN, ERA-I and MSG downwelling shortwave radiations with in situ measurements over the 12 October 2004–25 June 2012 period. Differences between the reanalysis estimates and the local measurements are computed at hourly time scale for SAFRAN and MSG and at 3 h time scale for ERA-I. In the MSG figure, the white lines correspond to missing data. On the *y* axis, "Jan" and "Jul" stands for January and July. The two digits indicate the year.

GMDD
8, 2053–2100, 2015

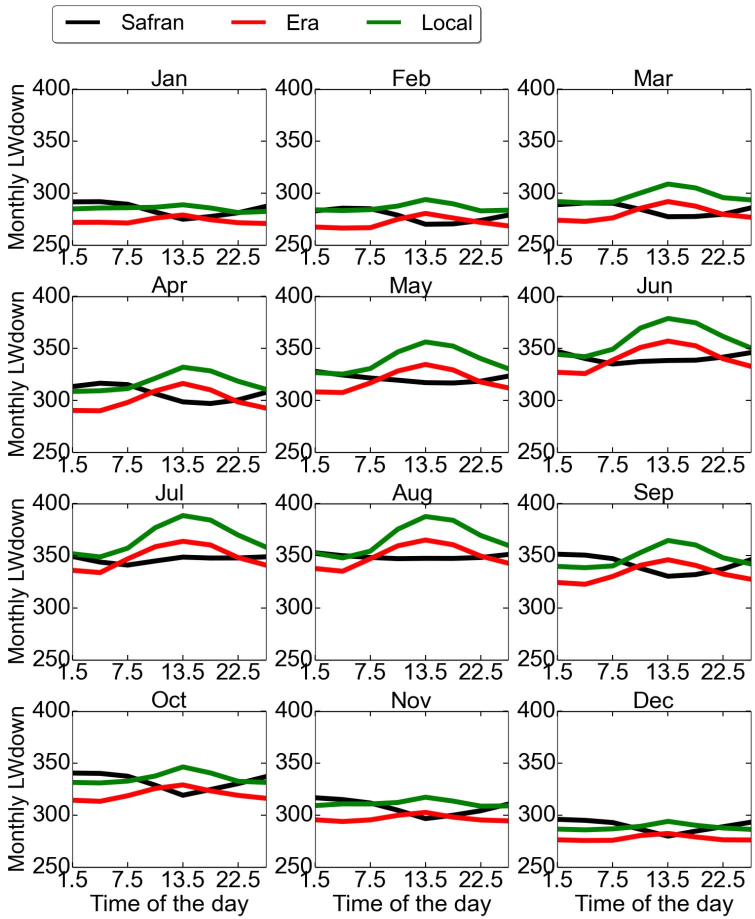

Figure 5. Comparison of SAFRAN, ERA-I and in situ mean monthly downwelling longwave radiation (LWdown in $W m^{-2}$) over the 25 April 2001–25 June 2012 period. The estimates correspond to 3 h integrated values.

GMDD
8, 2053–2100, 2015

GMDD
8, 2053–2100, 2015

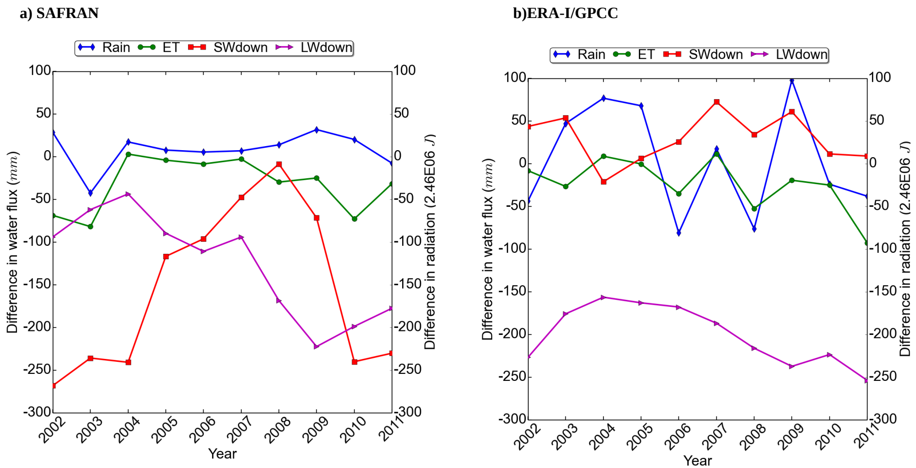

Figure 6. Impact of meteorological reanalysis on yearly budgets: Yearly values of downwelling shortwave radiation (SWdown), downwelling longwave radiation (LWdown), rainfall and simulated evapotranspiration (ET) are evaluated for the SAFRAN **(a)** and ERA-I/GPCC **(b)** reanalyses. For radiations and rainfall, the differences in yearly cumulative values between the reanalysis variable and the local observation are represented. For ET, the differences in yearly cumulative values between the simulation based on the reanalysis climate (S_{SAF} and S_{ERA}) and the simulation achieved with the local climate (S_{irri}) are shown. The radiation unit is given in 2.46×10^6 J to match the water flux scale given in mm (1 mm of ET is equivalent to $\sim 2.46 \times 10^6$ J where 2.46×10^6 is an approximation of the latent heat for vaporization of water).

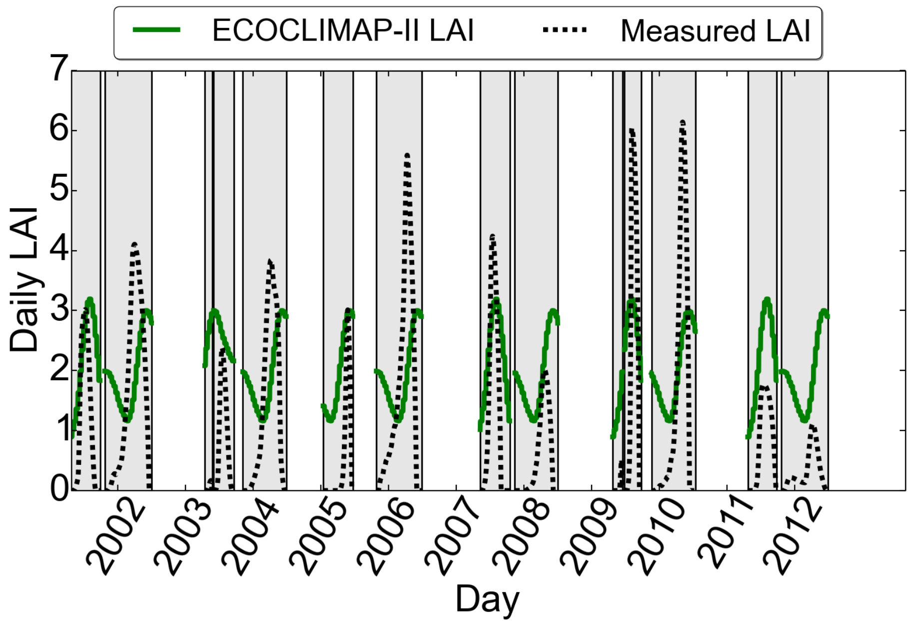

Figure 7. Comparison of the Ecoclimap-II LAI with the in situ LAI over the crop cycles of the 12 year crop succession. Crop and inter-crop periods are represented by grey and white background, respectively.

GMDD
8, 2053–2100, 2015

Impact of forcing variables on ISBA-A-gs simulation of ET

S. Garrigues et al.

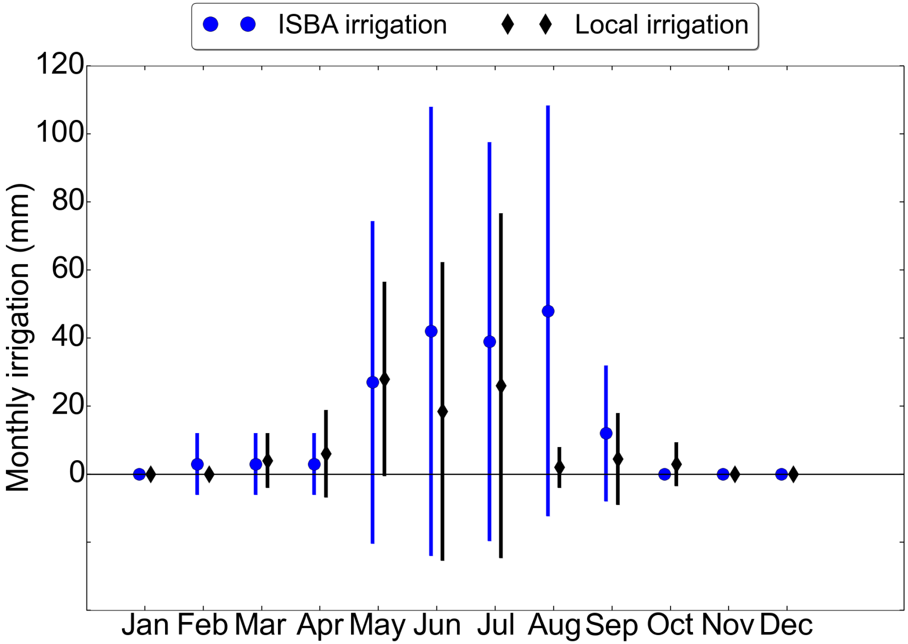

Figure 8. Comparison of the local and simulated mean monthly cumulative irrigation amount. The vertical bars represent the inter-annual variability (± one SD). The total cumulative value of in situ and simulated irrigation over 12 years are 1295 and 2070 mm, respectively.

GMDD
8, 2053–2100, 2015

Impact of forcing variables on ISBA-A-gs simulation of ET

S. Garrigues et al.